ENVIRONMENTAL RESEARCH
LETTERS

LETTER • OPEN ACCESS

Accounting for internal migration in spatial population projections—a gravity-based modeling approach using the Shared Socioeconomic Pathways

To cite this article: Lena Reimann *et al* 2021 *Environ. Res. Lett.* **16** 074025

IOP Publishing Environ. Res. Lett. 16 (2021) 074025 https://doi.org/10.1088/1748-9326/ac0b66

ENVIRONMENTAL RESEARCH
LETTERS

OPEN ACCESS

RECEIVED
30 December 2020

REVISED
26 March 2021

ACCEPTED FOR PUBLICATION
15 June 2021

PUBLISHED
1 July 2021

LETTER

Accounting for internal migration in spatial population projections—a gravity-based modeling approach using the Shared Socioeconomic Pathways

Lena Reimann[1,2,4,*], **Bryan Jones**[2], **Theodore Nikoletopoulos**[3] **and Athanasios T Vafeidis**[1]

[1] Department of Geography, Kiel University, Ludewig-Meyn-Straße 14, 24118 Kiel, Germany
[2] CUNY Institute for Demographic Research (CIDR), City University of New York, 135 E 22nd St, New York City, NY 10010, United States of America
[3] Department of Biophysics, Radboud University, 6525AJ Nijmegen, The Netherlands
[4] Institute for Environmental Studies (IVM), Vrije Universiteit Amsterdam, De Boelelaan 1111, 1081 HV Amsterdam, The Netherlands
[*] Author to whom any correspondence should be addressed.

E-mail: lena.reimann@vu.nl

Keywords: high-resolution gridded population projections, gravity-based population downscaling model, urban sprawl, inland-coastal migration, shared socioeconomic pathways (SSPs), Mediterranean region

Supplementary material for this article is available online

Abstract

Gridded population projections constitute an essential input for climate change impacts, adaptation, and vulnerability (IAV) assessments as they allow for exploring how future changes in the spatial distribution of population drive climate change impacts. We develop such spatial population projections, using a gravity-based modeling approach that accounts for rural-urban and inland-coastal migration as well as for spatial development patterns (i.e. urban sprawl). We calibrate the model (called *CONCLUDE*) to the socioeconomically diverse Mediterranean region, additionally considering differences in socioeconomic development in two geographical regions: the northern Mediterranean and the southern and eastern Mediterranean. We produce high-resolution population projections (approximately 1 km) for 2020–2100 that are consistent with the Shared Socioeconomic Pathways (SSPs), both in terms of qualitative narrative assumptions as well as national-level projections. We find that future spatial population patterns differ considerably under all SSPs, with four to eight times higher urban population densities and three to 16 times higher coastal populations in southern and eastern Mediterranean countries compared to northern Mediterranean countries in 2100. In the South and East, the highest urban density (8000 people km^{-2}) and coastal population (107 million) are projected under SSP3, while in the North, the highest urban density (1500 people km^{-2}) is projected under SSP1 and the highest coastal population (15.2 million) under SSP5. As these projections account for internal migration processes and spatial development patterns, they can provide new insights in a wide range of IAV assessments. Furthermore, *CONCLUDE* can be extended to other continental or global scales due to its modest data requirements based on freely available global datasets.

1. Introduction

The future impacts of climate change will be driven by physical changes in climatic conditions as well as by changes in socioeconomic development (Field *et al* 2014). Recent studies found that socioeconomic development can be the dominant factor in driving impacts, in particular in the first half of the 21st century when climatic changes still take place at a slower pace (Marsha *et al* 2018, Rohat *et al* 2019c) and in regions with rapid population growth (Brown *et al* 2018, Jones *et al* 2018, Monaghan *et al* 2018, Rohat *et al* 2019a). To assess future impacts in a comprehensive manner, it is therefore important to explore the range of uncertainty regarding changes in socioeconomic conditions in locations that are exposed to climate hazards (Moss *et al* 2010, Ebi *et al* 2014).

The current state-of-the-art socioeconomic scenarios in climate change research, the Shared Socioeconomic Pathways (SSPs), provide a suitable basis for exploring this uncertainty (O'Neill *et al* 2014, 2020). Five global-scale SSPs describe plausible alternative trends in socioeconomic development in the course of the 21st century based on societal challenges to climate change mitigation and adaptation. Each SSP has an underlying narrative that describes the socioeconomic developments of the SSP in qualitative terms (O'Neill *et al* 2017; SM1); furthermore, the narratives have been quantified to produce national-level projections of key variables in impacts, adaptation, and vulnerability (IAV) research (Van Ruijven *et al* 2014) such as population (Kc and Lutz 2017), urbanization (Jiang and O'Neill 2017), and gross domestic product (Crespo Cuaresma 2017, Dellink *et al* 2017, Leimbach *et al* 2017).

However, national-level projections can be applied in IAV research to a limited degree as these assessments require spatially downscaled projections of key variables (Van Vuuren *et al* 2010, Van Ruijven *et al* 2014), with population being one of the most-used indicators for characterizing future impacts, for instance with regard to heat stress (Jones *et al* 2015, Rohat *et al* 2019a), water scarcity (Hanasaki *et al* 2013, Veldkamp *et al* 2016, Chen *et al* 2018), river flooding (Jongman *et al* 2015, Winsemius *et al* 2016), and coastal flooding (Hinkel *et al* 2014, Neumann *et al* 2015, Tiggeloven *et al* 2020). A number of previous studies have spatially downscaled population projections to the grid cell level, using the national-level SSP projections as boundary conditions, for example at global scale (Jones and O'Neill 2016, Murakami and Yamagata 2019), with a focus on coastal population growth (Merkens *et al* 2016); at continental scale, for Africa (Boke-Olén *et al* 2017), Europe (Lückenkötter *et al* 2017, based on Batista E Silva *et al* 2016), and the Mediterranean region (Reimann *et al* 2018); and at national scale, for the US (Zoraghein and O'Neill 2020a, 2020b) and China (Chen *et al* 2020).

Besides their different regional contexts, these gridded population projections differ in terms of spatial resolution, input data, and modeling approaches used. The spatial resolution of the projections ranges from 100 m (Chen *et al* 2020) to 0.5° (Murakami and Yamagata 2019), depending on the complexity of the modeling approach, the intended application of the projections, and the regional focus of the study. Modeling approaches range from simple rescaling techniques (Lückenkötter *et al* 2017) to more data-intensive approaches using distance measures from existing settlements, roads, and other infrastructure as modeling variables (Boke-Olén *et al* 2017, Murakami and Yamagata 2019, Chen *et al* 2020). The approach of Merkens *et al* (2016) (also used in Reimann *et al* 2018) employs a rescaling technique that differentiates population development in coastal versus inland locations. However, it does not include spatial changes in settlement patterns (i.e. urban sprawl), which are accounted for in the gravity-based approach used by Jones and O'Neill (2016) (also used in Zoraghein and O'Neill 2020a, 2020b). The approaches of Merkens *et al* (2016) and Jones and O'Neill (2016) have modest data requirements, primarily relying on spatial population distributions of two time steps as model input; therefore both approaches are suitable for applications at continental to global scales where consistent input data are often lacking (Vafeidis *et al* 2008, Leyk *et al* 2019).

None of the above-mentioned approaches account for both urban development patterns and inland-coastal migration, although these two processes are considered key drivers of future climate change impacts, in particular in coastal locations (Seto *et al* 2011, Neumann *et al* 2015, Merkens *et al* 2018). Historically, coastal locations have experienced high population growth, resulting in higher population densities and urbanization levels compared to inland locations (McGranahan *et al* 2007, Kummu *et al* 2016). Accordingly, the majority of megacities (>8 million inhabitants) are located in low-lying coastal areas (Brown *et al* 2013). With urbanization projected to increase in the course of the 21st century under all SSPs (Jiang and O'Neill 2017), these settlement patterns are expected to continue in the future (Nicholls *et al* 2008, Merkens *et al* 2016).

We address this gap by extending the gravity-based approach of Jones and O'Neill (2016) to account for distinct changes in settlement patterns (i.e. urban sprawl) in coastal versus inland locations; we name the extended version of the model *CONCLUDE*[4]. For capturing inland-coastal as well as rural-urban migration processes, we refine the spatial resolution from a resolution of 7.5 arc minutes (approximately 15 km at the equator) to 30 arc seconds (approximately 1 km). We use freely available global-scale input data to calibrate the model to observed changes in spatial population patterns in coastal and inland locations, using the Mediterranean region, a socioeconomically diverse region characterized by a densely populated and highly urbanized coastal zone (European Environment Agency 2014, Lange *et al* 2020), as a case study.

This regional focus allows us to calibrate the model to two geographical regions based on the largest current differences in socioeconomic development across the region, the northern[5] and

[4] The model of Jones and O'Neill (2016) has recently been referred to as *INCLUDE* (Jones 2020). To reflect that our model extension accounts for inland-coastal migration, we name our extended version of the model *CONCLUDE* (i.e. *CO*astal i*NCLUDE*).

[5] Northern Mediterranean countries include Andorra, Croatia, Cyprus, France, Greece, Italy, Malta, Monaco, San Marino, Slovenia, Spain, The Vatican, and the British overseas territory Gibraltar.

the southern and eastern[6] Mediterranean (Reimann *et al* 2018). Based on the calibrated model parameters for the two geographical regions and coastal versus inland locations, we produce gridded population projections in ten-year time steps from 2020 to 2100 for each SSP that reflect the development patterns described in the SSP narratives. These projections explore the uncertainty space regarding plausible future population patterns, and can be used in a wide range of IAV assessments.

In the methods section, we describe the modeling approach in more detail, including model calibration, validation, and modifications made to produce the population projections. In the results section, we present the spatial population patterns by SSP and geographical region, focusing particularly on developments in urban population density and in coastal population across the SSPs and the 21st century. We then critically evaluate the model for producing meaningful spatial population projections in the context of IAV research by comparing our results to previous work and by reflecting upon the model limitations. Last, we conclude with ideas of how to further refine the model in future work.

2. Methods

The following sections provide an overview of the extensions implemented in the gravity-based model *CONCLUDE* to be able to produce spatial population projections that account for spatial development patterns (i.e. urban sprawl) as well as for rural-urban and inland-coastal migration. Please consult supplementary materials 2–7 available online at stacks.iop.org/ERL/16/074025/mmedia for further methodological detail (as referenced in the text).

2.1. Modeling approach

We used and extended the gravity-based population model *INCLUDE* described in Jones and O'Neill (2013), Jones and O'Neill (2016) and Rigaud *et al* (2018). Demographic gravity models are based on Newton's law of gravity and gravitational potential, assuming that densely populated locations are more attractive for human settlement than less densely populated locations (so-called 'population potential' (Grübler *et al* 2007)), and that relative attractiveness decreases with increasing distance between locations (Anderson 2011). The basic notion underlying this assumption is that factors such as transport costs and travel times determine the spatial interaction of two places, which decreases with increasing distance (Rich 1980). This effect is called 'distance-decay' and is often represented with a negative exponential function (Skov-Petersen 2001, Iacono *et al* 2008).

In addition to the distance-decay effect, we accounted for the contribution of local characteristics to the attractiveness of a location. Accordingly, we calculated a population potential v for each grid cell i and time step t that represents the attractiveness of any given location:

$$v_i(t) = l_i \left(\sum_{j \in N_i} P_j(t)\, e^{-\beta d_{ij}} + A_i P_i(t) \right) \qquad (1)$$

where l_i is the proportion of cell i available for human settlement[7], P is the population of cell j or i at time t, β is a parameter reflecting the strength of the distance-decay effect, d_{ij} is the distance between cells i and j, and A_i is a factor reflecting the local attractiveness of cell i. The number of neighboring cell indices N_i is determined by the gravity window within which the distance-decay effect applies.

We calculated $v_i(t)$ separately for urban and rural populations, based on unique urban and rural β parameters for coastal and inland locations[8], and distinct gravity windows for the two geographical regions (see next section for further detail). We then spatially distributed the national-level population of $t+1$ to each grid cell proportional to $v_i(t)$.

2.2. Calibration

The model was calibrated to historical changes in population patterns; therefore, spatial population data for at least two time steps were required. We used the global human settlement layer (Florczyk *et al* 2019) population data (GHS-POP) of the years 1990, 2000, and 2015, available at a spatial resolution of 30 arc seconds (WGS84 coordinates) (Schiavina *et al* 2019). GHS-POP was developed by spatially distributing the population of the Gridded Population of the World (GPW) (Center for International Earth Science Information Network—CIESIN—Columbia University 2017) based on built-up area identified with the help of satellite imagery for each time step (Freire *et al* 2016). As we calibrated the model to two ten-year time steps (i.e. 1990–2000; 2000–2010), we established the population distribution of 2010 by linearly interpolating the GHS-POP data of the years 2000 and 2015.

Following Jones and O'Neill (2016), we calibrated the model separately to urban versus rural changes in population patterns. Therefore, we defined the urban population per grid cell using the GHS-based settlement model (GHS-SMOD) (Florczyk *et al* 2019, Pesaresi *et al* 2019). To harmonize the total urban population per country based on GHS-SMOD with the UN World Urbanization Prospects' (WUP) urbanization level for each country (United Nations,

[6] Southern and eastern Mediterranean countries include Algeria, Albania, Bosnia and Herzegovina, Egypt, Israel, Lebanon, Libya, Montenegro, Morocco, Palestine, Syria, Tunisia, and Turkey.

[7] Please see SM2 for a description of how the spatial mask (l_i) was produced.

[8] Please see SM3 for a description of the coastal zone definition used in this study.

Department of Economic and Social Affairs, Population Division 2019), we added (deducted) population from densely populated neighboring grid cells to (from) the urban population in a series of three steps until the urban population numbers matched those of the WUP (SM4).

We established the distance parameter β for urban and rural locations by minimizing the sum of the squared errors produced by the model at the grid cell level for each ten-year calibration period, following Jones and O'Neill (2016). As not all countries were equally suitable for this procedure due to differences in the currency and spatial detail of the census and administrative unit data underlying GHS-POP (Center for International Earth Science Information Network—CIESIN—Columbia University 2017), we selected one country per geographical region (i.e. Spain, Tunisia) as representative of the migration processes in the region. We tested different gravity windows for each region, assuming that (a) daily trip distances in the Mediterranean are shorter than the 100 km window used by Jones and O'Neill[9], and (b) daily trip distances are shorter in the southern and eastern Mediterranean compared to the northern Mediterranean, using the lower motorization rate as a proxy for trip distances (Eurostat 2019) due to a lack of consistent region-wide data. We found a gravity window of 20 km for the northern and 10 km for the southern and eastern parts of the region to best reflect the distance-decay effect. Finally, we averaged the established urban and rural β parameters across the two calibration periods and modified them to be able to account for differences in population development patterns in coastal versus inland locations (SM5).

In a next step, we calculated the local attractiveness factor A_i in urban and rural locations for each country and grid cell by eliminating the grid-cell error ε_i produced when accounting for the distance-decay effect only. Therefore, we ran equation (1) for the calibration period, applying the established coastal rural (CR), inland rural (IR), coastal urban (CU), and inland urban (IU) β parameters in the respective settlement type (i.e. CR, IR, CU, IU). As A_i attained extremely high (low) values in some cells, we applied a two-step post-processing approach. First, to remove outliers, we used the middle 50% (so-called interquartile range) of the A_i distribution per country. Second, we scaled A_i to values ranging from -100 to 100, while retaining the original distribution of A_i per country. Using this approach, we avoided overfitting the model to the historical changes in population patterns observed during the calibration period.

[9] Jones and O'Neill (2013) established the gravity window size based on daily trip distances in the US (see their supplementary data).

2.3. Validation

We validated the model by projecting the 2010 population based on the calibration period 1990–2000. Figure 1 presents scatter plots of the modeled versus the observed population for the total population, for urban populations, and for rural populations (see SM6 for corresponding Q-Q plots). The plots illustrate better model performance for urban populations compared to rural populations, with the best performance achieved when combining urban and rural populations (panel a), as reflected in R^2 and the root mean squared error. These findings agree with the findings of Jones and O'Neill (2013). A map presenting the error per grid cell relative to the observed population per cell (=relative absolute error (RAE)) for the entire Mediterranean region can be found in SM6.

We calculated further error metrics for the region to evaluate model performance in rural (CR, IR) and urban (CU, IU) locations as well as the entire Mediterranean region (supplementary table 3). In the entire Mediterranean region, the model produced a mean absolute error of 6.6, and a weighted mean absolute percentage error (WMAPE) (weighted by the population) of 14.7%, which compared well with the original version of the model that produced a WMAPE of 11.6% at the US level (Jones and O'Neill 2013). These error metrics also illustrated better model performance in urban versus rural locations (WMAPE of 18.3% versus 34.4%) as well as in coastal versus inland locations (WMAPE of 30.9% in CR versus 35.7% in IR; 18% in CU versus 18.5% in IU).

2.4. Population projections

To produce downscaled population projections with *CONCLUDE* that are consistent with the SSPs, we used the national-level population (Kc and Lutz 2017) and urbanization (Jiang and O'Neill 2017) projections provided in the SSP database (International Institute for Applied Systems Analysis 2018) as boundary conditions. These projections differentiate developments in high-fertility, rich OECD low-fertility, and other low-fertility countries, and include assumptions on fertility, mortality, education levels, and international migration (Kc and Lutz 2017). To reflect the future spatial development patterns per SSP, we modified the calibrated β parameters for each SSP by interpreting the qualitative assumptions described in the global SSP narratives (Jiang and O'Neill 2017, O'Neill *et al* 2017) and the Mediterranean coastal SSP narratives (Reimann *et al* 2018), and by conducting a sensitivity analysis (SM7). Additionally, we applied SSP-specific population density thresholds per grid cell based on the observed maximum population density of 2015, and accounted for future changes in habitability under the SSPs by adjusting the spatial mask l_i. Finally, we produced population projections in ten-year time steps from 2020 to 2100 and for each SSP by modeling urban and

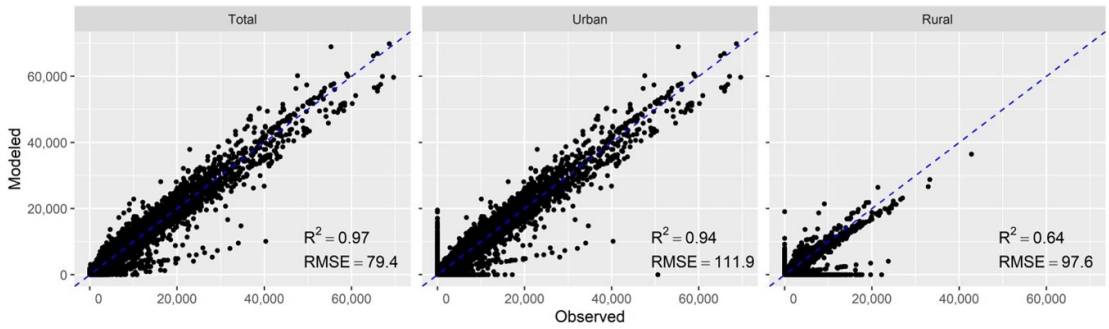

Figure 1. Scatter plots of the total population, urban populations, and rural populations, along with R^2 and the root mean squared error (RMSE). Blue line represents the perfect fit.

rural populations separately based on the respective coastal and inland β parameters. We further redefined some rural and urban population cells after each time step based on population density and contiguity (following Jones and O'Neill 2016) before combining them to obtain the total population.

3. Results

The spatial population projection datasets produced for each SSP and ten year time step are publicly available at Reimann *et al* 2021 The following sections first describe the spatial population patterns per SSP and then provide a more detailed description of the urban as well as coastal population patterns in the two geographical regions.

3.1. Spatial population patterns

Figure 2 presents a selected set of the population projections, including the baseline distribution (2010) along with each SSP in 2100. These spatial population patterns reflect the national-level population (Kc and Lutz 2017) and urbanization projections (Jiang and O'Neill 2017) (SM8) as well as the qualitative assumptions regarding spatial development patterns described in each SSP (O'Neill *et al* 2017). In SSP1, countries experience rapid urbanization, with urbanization levels of around 95% (2100) across the entire region. Effective management combined with population decline in the second half of the century results in high-density, compact urban settlements. In SSP2, urbanization is less rapid, with higher urbanization levels in the northern parts of the region (ca. 93%) compared to the South and East (roughly 85%). Population growth is mixed across countries and spatial development is slightly more concentrated than observed in historical patterns, leading to urban sprawl in countries with high urbanization levels and a growing population (e.g. France, Israel). SSP3 is characterized by low urbanization rates, with urbanization levels of roughly 84% in the northern Mediterranean and 65% in the southern and eastern Mediterranean. Population declines in almost all northern countries and increases rapidly in southern and eastern countries, resulting in sprawling development in the South and East. In SSP4, urbanization increases rapidly, with urbanization levels of around 93% across the region. Population decreases in most countries, notable exceptions being France and countries of the Middle East, where high urban sprawl can be observed until 2100. SSP5 is characterized by urbanization levels similar to those in SSP1, combined with rapid population growth in northern countries and the Middle East, which leads to considerable urban sprawl, particularly in northern parts of the region.

3.2. Urban population density

The population development patterns described in section 3.1 are further illustrated in figure 3 which presents urban population densities per SSP and geographical region. In the baseline year (2010), urban population density is about four times higher in southern and eastern Mediterranean countries than in countries of the Mediterranean North (figure 3(a)); this difference is projected to increase until 2100 under all SSPs, with the largest difference in SSP3, where urban settlements are projected to be eight times more densely populated in the South and East. In northern countries, urban population density increases in SSP1 and decreases in all other SSPs in 2100, compared to the baseline. The highest urban population density (1600 people km^{-2}) is projected in SSP1 and the lowest density of roughly 700 people km^{-2} in SSP5. These results reflect the continuation of high urban sprawl (except in SSP1), in combination with population decline in the second half of the century in SSPs 1–4. In the South and East, urban population density increases in SSPs 1–3 and decreases in SSPs 4 and 5 until 2100, compared to 2010. The highest urban population density of over 8000 people km^{-2} is projected in SSP3, the scenario with the highest expected population growth in these countries; the lowest density of ca. 4150 people km^{-2} is projected under SSP4.

Figure 3(b) presents the development of urban population densities in the course of the century,

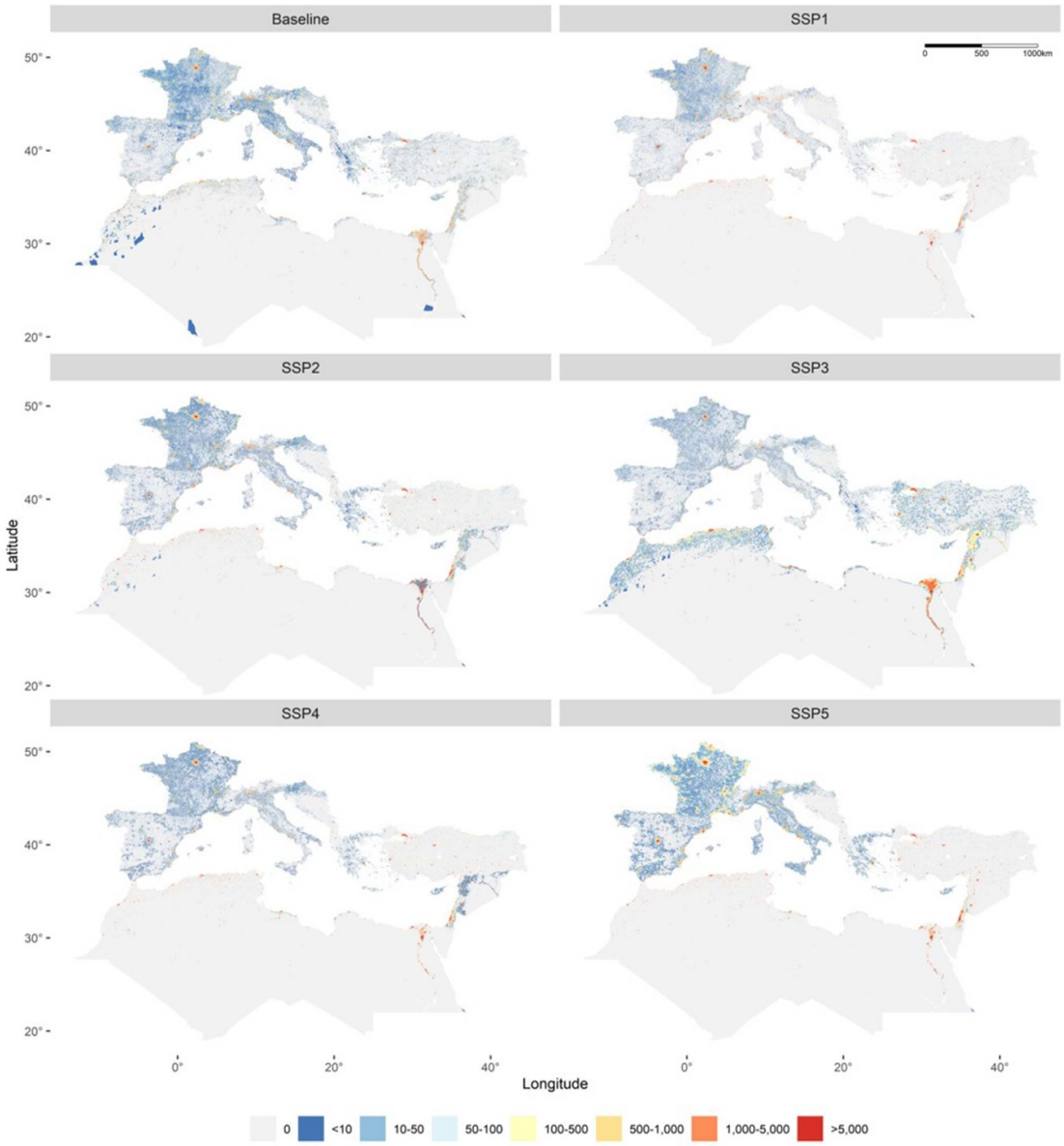

Figure 2. Population per grid cell in the baseline year (2010) and for each SSP in 2100. Resolution: 30 arc seconds (WGS84).

differentiating between coastal and inland locations. In both geographical regions, density is higher in coastal locations compared to inland locations under all SSPs and time steps except the base year. In the Mediterranean North, urban population density in coastal locations first increases in SSPs 1–4, before it decreases in the second half of the century; in inland locations, density decreases in the course of the century in all SSPs except SSP1 where it first increases and starts to decrease in 2080. In the South and East, urban population density increases in coastal and inland locations under SSPs 1–3, with a rapid increase in coastal locations, which levels off in SSP1 from 2080 onwards. Under SSPs 4 and 5, urban population density experiences some increase in coastal locations until 2070 and remains on a similar level in inland locations in the course of the century.

3.3. Coastal population

Comparing the population in coastal locations across SSPs and geographical regions (figure 4), we observe, similar to urban population density, a population three orders of magnitude higher in coastal locations in southern and eastern countries compared to the Mediterranean North in 2010 (figure 4(a)). This difference is projected to increase until 2100 under all SSPs except SSP5 where coastal population increases considerably in the northern Mediterranean as well, resulting in the highest coastal population (15.2 million) in 2100. Further, the number of people in coastal locations in the North increases slightly in SSP1 and SSP2 and decreases in SSPs 3 and 4 compared to the baseline, with the lowest number of roughly 6.5 million people in coastal locations under SSP3. In the South and East, we observe the

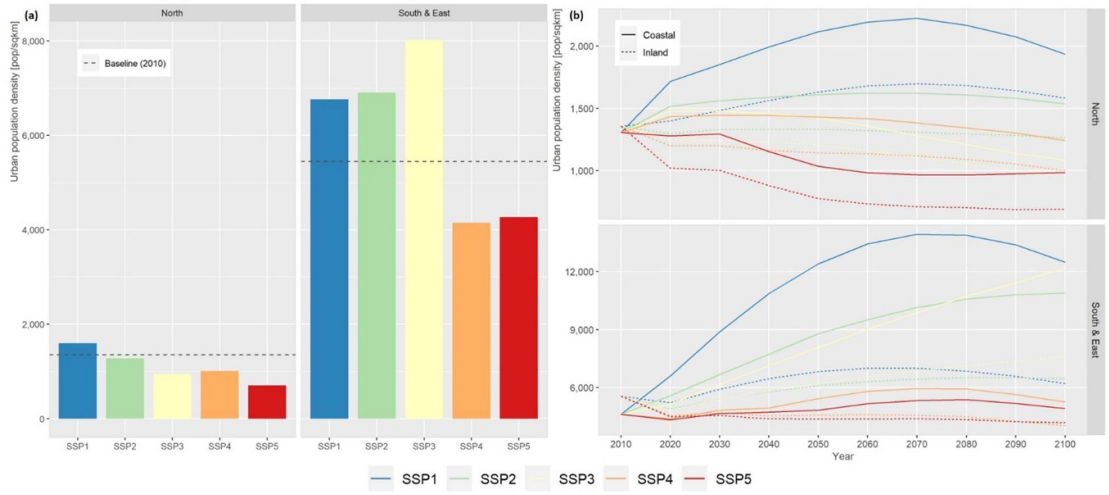

Figure 3. Urban population density in each SSP and geographical region (a) in 2100 compared to 2010, (b) development 2010–2100 in coastal versus inland locations. Coastal = low elevation coastal zone (see SM3; McGranahan et al 2007). Please note different scales of the y-axes.

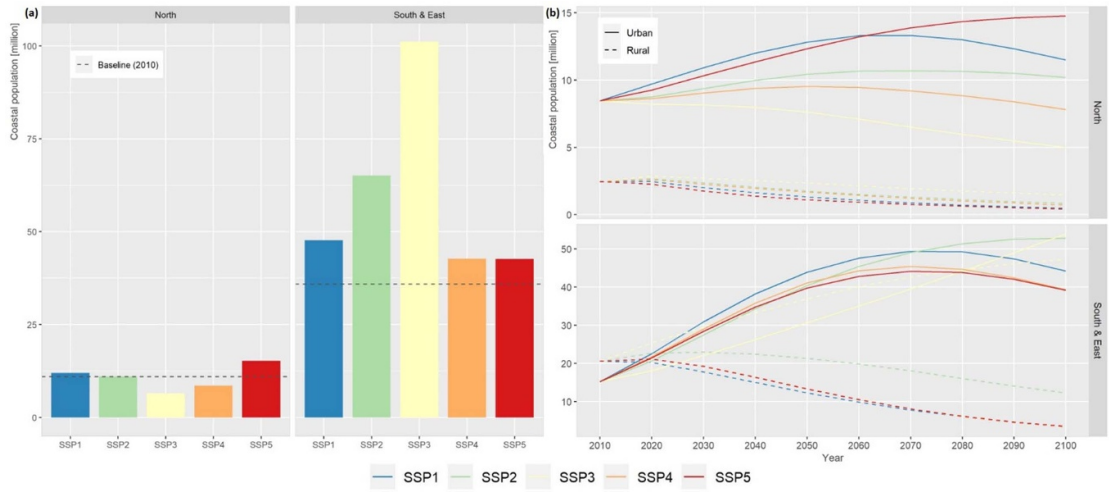

Figure 4. Coastal population in each SSP and geographical region (a) in 2100 compared to 2010, (b) development 2010–2100, differentiating urban versus rural populations. Coastal = low elevation coastal zone (see SM3; McGranahan et al 2007). Please note different scales of the y-axes.

opposite development: the highest coastal population of over 100 million in 2100 is projected under SSP3, whereas we find the lowest coastal population of ca. 42.7 million under SSP5. Nonetheless, the number of people in coastal locations of southern and eastern countries increases under all SSPs compared to the baseline. These results reflect the higher attractiveness of coastal locations compared to inland locations in both geographical regions, which is amplified in the southern and eastern Mediterranean by a limited land area available for human settlement in inland locations (SM2), and superimposed by country-level population decline in the northern Mediterranean under SSPs 3 and 4 (SM8).

In figure 4(b), the development of the coastal population in the course of the century is shown for urban versus rural populations. In the northern Mediterranean, the coastal population lives primarily in urban settlements under all SSPs. It first increases under all SSPs except SSP3, where it decreases gradually in the course of the century. In the second half of the century, the urban population in coastal locations also declines in SSPs 1, 2, and 4. The coastal population in rural settlements decreases slowly under all SSPs. In southern and eastern countries, a similar share of the coastal population lives in urban and rural settlements in 2010, which changes considerably until 2100, when the vast majority of people in coastal locations are projected to live in urban settlements under all SSPs except SSP3. Urban population in coastal locations increases markedly under all SSPs and starts to decline in 2080 under SSPs 1, 4, and 5. The coastal population in rural settlements continuously increases under

SSP3 until 2100, and gradually decreases under all other SSPs, in particular in the second half of the century.

4. Discussion

Our spatially downscaled population projections account for important migration processes within countries (i.e. rural-urban and inland-coastal) as well as for plausible future spatial development patterns (i.e. urban sprawl). As such they constitute improved representations of future population distributions and are useful for a wide range of IAV assessments. The spatial resolution (30 arc seconds) is suitable for capturing these development trends and patterns while avoiding a misleading impression of certainty as future socioeconomic developments are highly uncertain (Preston *et al* 2011, Sherbinin *et al* 2019). Therefore, we anticipate that the developed projections are particularly meaningful for assessments at continental to regional scales, for example for analyzing exposure to extreme heat, water scarcity, and flooding (coastal, fluvial, pluvial). In such assessments, it is important to consider different SSPs in order to represent the range of uncertainty in future exposure. The insights of these assessments can support decision-making by identifying hotspots of future exposure where adaptation is urgently needed. Therefore, decisions can be made that are robust under a wide range of plausible futures (Moss *et al* 2010, Walker *et al* 2013, Haasnoot *et al* 2020). However, to inform local-scale decisions such as the implementation of specific adaptation measures, more refined modeling approaches are needed that allow for integrating local characteristics based on more refined scenario assumptions (e.g. Reimann *et al* 2021) and more detailed input data to further downscale the developed population projections (e.g. Merkens and Vafeidis 2018).

Our results suggest higher future climate change exposure in southern and eastern Mediterranean countries compared to northern Mediterranean countries due to consistently higher urban densities and coastal population under all SSPs. However, exposure would differ markedly across SSPs, depending on the socioeconomic challenges for adaptation that result from differences in the effectiveness of policies and institutions, economic growth, and technological change among others (O'Neill *et al* 2017). Assuming that an increase in urban population density increases the urban heat island (UHI) effect, therefore leading to higher urban heat stress, which will exacerbate due to climate change (Chapman *et al* 2017, Koomen and Diogo 2017, Vanos *et al* 2020), heat exposure would be highest under SSP3 in the South and East and SSP1 in the North. As SSP1 is characterized by sustainable development with well-managed, compact urban areas and low adaptation challenges, it would result in potentially lower exposure than SSP3 (assuming all else equal), as SSP3 is characterized by high adaptation challenges due to slow economic growth, low technological development, and weak policies and institutions. Similarly, coastal exposure would be highest in the South and East under SSP3, with a large share of the coastal population living in rural settlements, where coastal protection is expected to be rarely pursued as costs often exceed benefits (Lincke and Hinkel 2018). In the North, coastal exposure would be highest under SSP5 and SSP1, which are both characterized by low adaptation challenges. Due to high urban sprawl in SSP5, we expect coastal adaptation to be more challenging than in SSP1. Furthermore, as SSP5 experiences rapid economic growth, residual risk would be high, leading to high damages in case of adaptation failure during coastal flooding. While we are aware that the future lies somewhere between (or even beyond) the five SSPs (O'Neill *et al* 2017, 2020), our results suggest that future spatial population patterns will contribute to higher exposure in the southern and eastern Mediterranean, which may exacerbate already existing disparities between the two geographical regions (MedECC 2020).

To be able to further contextualize these results, the population projections can be enriched by additional demographic and socioeconomic variables important for IAV research, such as age, sex, race, education, poverty, and income. Such extensions are limited in the current literature, with few examples that have downscaled IAV variables with the help of SSP-based population projections at national (i.e. the US) (Hauer 2019, Jiang *et al* 2020), European (Hurth *et al* 2017, Rohat *et al* 2019b), and global scales (Murakami and Yamagata 2019). Furthermore, our projections do not account for the potential impacts of climate change on migration, which is expected to increase once impacts such as flooding, heat stress, and droughts become more severe (Black *et al* 2011, McLeman 2019). To account for this effect, plausible future changes in climatic conditions based on the Representative Concentration Pathways (RCPs) (Van Vuuren *et al* 2011) can be integrated into the model to produce projections that account for climate change-induced migration, a first example being the work of Rigaud *et al* (2018). Such integrated assessments can additionally explore potential feedbacks between climate change, adaptation strategies, and migration patterns, which are expected to influence future impacts substantially (Aerts *et al* 2018). An aspect that we have not included in this study is the influence of shocks such as conflict, economic crises, or pandemics (e.g. COVID-19) on socioeconomic development as shocks are, by definition, not captured in the plausible[10] descriptions of the SSPs.

[10] Plausible developments are defined as developments that 'could happen' based on the current knowledge and understanding of the world (Voros 2003).

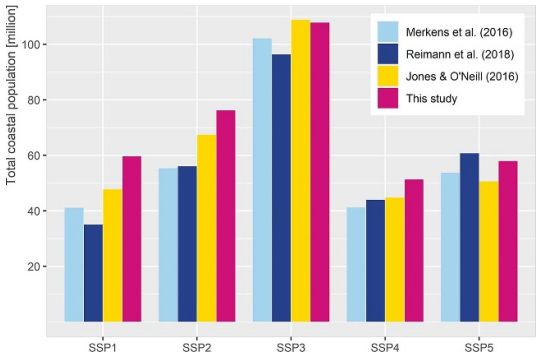

Figure 5. Mediterranean coastal population in 2100 based on Merkens et al (2016), Reimann et al (2018), Jones and O'Neill (2016) (downscaled projections of Gao 2017), and the approach used in this study. Coastal = low elevation coastal zone, based on MERIT DEM (Yamazaki et al 2017).

However, as we explore a large range of uncertainty by projecting spatial population patterns under the five SSPs, we assume that the effects of most shocks are covered by this uncertainty range, as pointed out by O'Neill *et al* (2020).

To evaluate the performance of the model in producing spatial population projections, we compared our results to those of previous work that accounted either for inland-coastal migration (Merkens *et al* 2016, Reimann *et al* 2018) or for urban sprawl (Jones and O'Neill 2016, downscaled by Gao 2017). As two studies do not provide projections that distinguish between urban and rural populations, we focus on the coastal population. We find that the population numbers projected in coastal locations in 2100 for each SSP are similar across the four studies, but also show marked differences (figure 5). Similar to Jones and O'Neill, we project the highest coastal population of 108 million in SSP3 and the lowest population of 51 million in SSP4. However, we project a 13%–25% higher coastal population than Jones and O'Neill under all SSPs except SSP3 where our projected population is 0.9% lower. These patterns reflect the higher attractiveness of coastal locations implemented in our approach, as established during model calibration (SM5). In SSP3, this effect is superimposed by rapid population decline in northern Mediterranean countries in SSP3 (section 3.1), which leads to a higher decline in coastal population in our approach compared to Jones and O'Neill as population decline takes place relative to attractiveness (i.e. more attractive locations experience higher decline). This potential model limitation needs further analysis which is currently inhibited by a lack of empirical evidence regarding the spatial patterns during phases of population decline (Grübler *et al* 2007, Jones and O'Neill 2013).

In contrast to our approach, the coastal approach of Merkens *et al* and Reimann *et al* projects the lowest coastal population of 41/35 million in SSP1, based on the assumption that the implementation of regulatory policies leads to sustainable and effective management of coastal areas, thereby reducing their attractiveness. The number of coastal inhabitants is about 30%–40% lower compared to our approach. This difference reflects one limitation of the gravity approach, which models aggregate population trends primarily based on the distance-decay effect (section 2.1) and does not account for the effects of policy on a location's attractiveness. Future work can integrate such effects into the model as an additional model layer similar to the spatial mask (l_i), in which the population potential in effectively managed locations could be set to 0. Further, SSP5 is the only scenario where the coastal approach results in roughly the same or a slightly higher number of coastal inhabitants (5%) as it assumes coastal locations to be very attractive, while not accounting for the sprawling development that we assume under SSP5.

Of the four approaches, our approach spans the narrowest uncertainty range across the SSPs with regard to the population projected in coastal locations in 2100 (i.e. 56.5 million versus 61.1–64 million), which suggests that accounting for several processes that drive spatial population patterns can reduce the range of uncertainty. As our approach results in the highest number of coastal inhabitants under almost all SSPs, we expect these results to be particularly meaningful from a risk-management perspective as strategies for reducing risk can be developed based on 'worst-case' conditions (Hinkel *et al* 2015). Comparison of the spatial population patterns projected under the four approaches further supports that our approach produces plausible results (supplementary figure 9). However, it also illustrates the limited comparability of the four modeling approaches due to different input data used, which result in distinct spatial population patterns.

When using our population projections, the following additional limitations need to be considered. First, we calibrated the model to a relatively short period of twenty years due to a lack of long-term gridded population data. This period was characterized by population growth in most Mediterranean countries. As we expect to see declining population numbers in the second half of the century under almost all SSPs, the observed changes in population patterns are not necessarily indicative of future patterns. Second, since we were not able to calibrate the β parameters for each country individually, the calibrated parameters may not reflect the spatial development patterns in all countries of the respective geographical region to the same degree. Similarly, we had to post-process the calibrated parameters to reflect differences in development patterns in coastal versus inland locations as our calibration procedure did not produce plausible parameters for these locations. We assume the reason for this being the small strip of land defined as coastal compared to its inland counterpart,

which may impede finding the optimal β parameter (section 2.2; SM5). Third, we would like to point out that the redefinition of grid cells into urban and rural populations after each projection time step (section 2.4) can follow a different algorithm than the one used in this study, one example being the 'degree of urbanization' (Pesaresi *et al* 2016).

More broadly, gravity-based models have several limitations that merit further discussion. First, the underlying assumption that densely populated locations are more attractive for human settlement than less densely populated locations results in higher population growth in large cities compared to smaller cities, although small- and medium-sized cities are expected to experience higher population growth in the next decades (Birkmann *et al* 2016, United Nations, Department of Economic and Social Affairs, Population Division 2019, Gao and O'Neill 2020). To account for this phenomenon, the population potential can be calculated conditional to the city size (i.e. the total number of people residing in an urban agglomeration), which could be implemented in the model in follow-up work. However, by applying the local attractiveness factor A_i and a population density threshold per grid cell (SM7), our approach produces more diverse spatial patterns than a basic gravity approach. Second, as population potential is calculated based on observed settlement patterns, these patterns consolidate in the future, and new settlements can only emerge under very specific conditions. While this limitation may result in implausible spatial population patterns in less developed countries that are expected to experience rapid population growth until 2100, we expect it to be negligible in the Mediterranean region as population is expected to decline in the second half of the century in most countries and SSPs; in those countries that will experience rapid growth (e.g. the MENA (Middle East and North Africa) region under SSP3) land available for human settlement is limited (supplementary figure 2); Mediterranean settlement patterns have developed since antiquity (Cazenave 2014), thereby giving reason to believe that new settlements are less likely to emerge.

Despite its limitations, *CONCLUDE* produces plausible distributions of future population patterns for each SSP, which can be updated once new knowledge and data become available. The model allows for integrating additional model layers (e.g. a policy layer) as a weight on the population potential (v_i), and can be extended to explore climate change-induced migration, for example by correlating the local attractiveness factor A_i to changes in environmental conditions with the help of spatial regression models (Rigaud *et al* 2018). Due to its modest data requirements, we expect the model to be particularly relevant for producing consistent projections in data-scarce regions like the Mediterranean region, where detailed region-wide data are often lacking (Lange *et al* 2020). As we rely on freely available global input data, the model can easily be extended to other continents, regions, or the global scale, given that sufficient computing resources are available.

5. Conclusion

This paper presents SSP-based gridded population projections that account for rural-urban and coastal-inland migration processes as well as for spatial changes in settlement patterns (i.e. urban sprawl), which have been produced with *CONCLUDE*, an extended gravity-based model specifically developed for this study. We apply the model to the Mediterranean region, accounting for distinct characteristics in northern versus southern and eastern Mediterranean countries. Our projections have a spatial resolution of 30 arc seconds, a temporal resolution of ten-year time steps (2020–2100), and are consistent with the five SSPs, both in terms of qualitative narrative assumptions as well as national-level population projections. These projections explore the range of uncertainty regarding plausible future spatial population patterns in the 21st century and are useful for a wide range of IAV assessments. The model can be extended to account for the effects of climate change or spatial policies on a location's attractiveness for human settlement. As the model has modest data requirements and is calibrated to freely available global input data, it can be extended to other continental and/or global scales.

Future work can further refine the modeling approach by addressing its limitations such as separately calibrating the model to coastal versus inland locations; selecting a larger set of countries for the β calibration; and calibrating the model separately to phases of population growth and decline. Such refinements can also include the use of higher-resolution input data to be able to produce meaningful results at regional to national scale. Suitable datasets may be WorldPop (Tatem 2017) or a higher-resolution version of GHS-POP (Schiavina *et al* 2019), which are available at spatial resolutions of 3 arc seconds and 9 arc seconds, respectively. Further, a systematic assessment of the model's sensitivity to different population input data, urban versus rural population classification algorithms, and the choice of β parameters would provide useful insights for model users. Moreover, the model can be extended for integrated assessments to explore feedbacks between climate change impacts, adaptation strategies, and migration processes. For such assessments, different SSPs, RCPs, and Shared Policy Assumptions (SPAs) (Kriegler *et al* 2014) can be combined, as envisaged as part of the SSP-RCP-SPA scenario framework (Van Vuuren *et al* 2014, O'Neill *et al* 2020). Additionally, future research can explore the potential of the model for producing spatial projections of other key variables in IAV research. Last, we would like to encourage use of the

developed population projections in Mediterranean IAV assessments.

Data availability statement

The data that support the findings of this study are openly available at Reimann *et al* 2021. These data include gridded population projections for each SSP and ten-year time step (2010–2100). The model scripts (R Core Team 2020) are available from the corresponding author upon reasonable request.

Acknowledgments

We would like to thank Nora Bieker for her support in the sensitivity analysis. This work was initiated as part of a doctoral scholarship funded by the Fulbright Association that allowed LR to work at CIDR during a six-month research visit. We further acknowledge financial support by the state of Schleswig-Holstein within the funding programme Open Access Publikationsfonds.

ORCID iDs

Lena Reimann https://orcid.org/0000-0002-9405-9147
Athanasios T Vafeidis https://orcid.org/0000-0002-3906-5544

References

Aerts J C J H, Botzen W J, Clarke K C, Cutter S L, Hall J W, Merz B, Michel-Kerjan E, Mysiak J, Surminski S and Kunreuther H 2018 Integrating human behaviour dynamics into flood disaster risk assessment *Nat. Clim. Change* **8** 193–9

Anderson J E 2011 The gravity model *Annu. Rev. Econ.* **3** 133–60

Batista E Silva F, Dijkstra L, Martinez P V and Lavalle C 2016 *Regionalisation of Demographic and Economic Projections: Trend and Convergence Scenarios from 2015 to 2060* (*EUR, Scientific and technical research series* vol 27924) (Luxembourg: Publications Office)

Birkmann J, Welle T, Solecki W, Lwasa S and Garschagen M 2016 Boost resilience of small and mid-sized cities *Nature* **537** 605–8

Black R, Adger W N, Arnell N W, Dercon S, Geddes A and Thomas D 2011 The effect of environmental change on human migration *Glob. Environ. Change* **21** S3–11

Boke-Olén N, Abdi A M, Hall O and Lehsten V 2017 High-resolution African population projections from radiative forcing and socio-economic models, 2000–2100 *Sci. Data* **4** 160130

Brown S, Nicholls R J, Goodwin P, Haigh I D, Lincke D, Vafeidis A T and Hinkel J 2018 Quantifying land and people exposed to sea-level rise with no mitigation and 1.5°C and 2.0°C rise in global temperatures to year 2300 *Earth's Future* **6** 583–600

Brown S, Nicholls R J, Woodroffe C D, Hanson S, Hinkel J, Kebede A S, Neumann B and Vafeidis A T 2013 Sea-level rise impacts and responses: a global perspective *Coastal Hazards Coastal Research Library* vol 6 ed C W Finkl (Berlin: Springer) pp 117–49

Cazenave A 2014 Anthropogenic global warming threatens world cultural heritage *Environ. Res. Lett.* **9** 051001

Center for International Earth Science Information Network—CIESIN—Columbia University 2017 Gridded population of the world, Version 4 (GPWv4): population count adjusted to match 2015 revision of UN WPP country totals, Revision 10 (Palisades, NY: NASA Socioeconomic Data and Applications Center (SEDAC))

Chapman S, Watson J E M, Salazar A, Thatcher M and McAlpine C A 2017 The impact of urbanization and climate change on urban temperatures: a systematic review *Landscape Ecol.* **32** 1921–35

Chen J, Liu Y, Pan T, Liu Y, Sun F and Ge Q 2018 Population exposure to droughts in China under 1.5 °C global warming target *Earth Syst. Dynam.* **9** 1097–106

Chen Y, Li X, Huang K, Luo M and Gao M 2020 High-resolution gridded population projections for china under the shared socioeconomic pathways *Earth's Future* **8** 849

Crespo Cuaresma J 2017 Income projections for climate change research: a framework based on human capital dynamics *Glob. Environ. Change* **42** 226–36

De Sherbinin A *et al* 2019 Climate vulnerability mapping: a systematic review and future prospects *WIREs Clim. Change* **10** e600

Dellink R, Chateau J, Lanzi E and Magné B 2017 Long-term economic growth projections in the shared socioeconomic pathways *Glob. Environ. Change* **42** 200–14

Ebi K L, Kram T, Van Vuuren D P, O'Neill B C and Kriegler E 2014 A new toolkit for developing scenarios for climate change research and policy analysis *Environ. Sci. Policy Sustain. Dev.* **56** 6–16

European Environment Agency 2014 Horizon 2020 Mediterranean report: toward shared environmental information systems—EEA-UNEP/MAP joint report (available at: www.eea.europa.eu/publications/horizon-2020-mediterranean-report) (Accessed 22 Feb 2021)

Eurostat 2019 European neighbourhood policy—South—transport statistics (available at: https://ec.europa.eu/eurostat/statistics-explained/index.php/European_Neighbourhood_Policy_-_South_-_transport_statistics#Road_transport) (Accessed 22 Feb 2021)

Field C B *et al* (ed) 2014 *Climate Change 2014: Impacts, Adaptation and Vulnerability: Part A: Global and Sectoral Aspects. Contribution of Working Group II to the Fifth Assessment Report of the Intergovernmental Panel on Climate Change* (Cambridge: Cambridge University Press)

Florczyk A *et al* 2019 *GHSL data package 2019:* public release GHS P2019 (EUR vol 29788) (Luxembourg: Publications Office of the European Union)

Freire S, MacManus K, Pesaresi M, Doxsey-Whitfield E and Mills J 2016 *Development of new open and free multi-temporal global population grids at 250 m resolution* (Geospatial Data in a Changing World; Association of Geographic Information Laboratories in Europe (AGILE). AGILE 2016)

Gao J 2017 *Downscaling global spatial population projections from 1/8-degree to 1-km grid cells* (NCAR Technical Note NCAR/TN-537+STR, National Center for Atmospheric Researcher, Boulder, CO: USA)

Gao J and O'Neill B C 2020 Mapping global urban land for the 21st century with data-driven simulations and shared socioeconomic pathways *Nat. Commun.* **11** 2302

Grübler A, O'Neill B, Riahi K, Chirkov V, Goujon A, Kolp P, Prommer I, Scherbov S and Slentoe E 2007 Regional, national, and spatially explicit scenarios of demographic and economic change based on SRES *Technol. Forecast. Soc. Change* **74** 980–1029

Haasnoot M, Biesbroek R, Lawrence J, Muccione V, Lempert R and Glavovic B 2020 Defining the solution space to accelerate climate change adaptation *Reg. Environ. Change* **20** 305

Hanasaki N *et al* 2013 A global water scarcity assessment under shared socio-economic pathways—Part 2: water availability and scarcity *Hydrol. Earth Syst. Sci.* **17** 2393–413

Hauer M E 2019 Population projections for U.S. counties by age, sex, and race controlled to shared socioeconomic pathway *Sci. Data* **6** 190005

Hinkel J, Jaeger C, Nicholls R J, Lowe J, Renn O and Peijun S 2015 Sea-level rise scenarios and coastal risk management *Nat. Clim. Change* **5** 188–90

Hinkel J, Lincke D, Vafeidis A T, Perrette M, Nicholls R J, Tol R, Marzeion B, Fettweis X, Ionescu C and Levermann A 2014 Coastal flood damage and adaptation costs under 21st century sea-level rise *Proc. Natl Acad. Sci. USA* **111** 3292–7

Hurth F, Lückenkötter J and Schonlau M 2017 European GDP projections for 2015–2060-10km gridded data based on Shared Socioeconomic Pathways (SSPs) (IRPUD, TU Dortmund)

Iacono M, Krizek K and El-Geneidy A M 2008 Access to destinations: how close is close enough? Estimating accurate distance decay functions for multiple modes and different purposes (available at: https://conservancy.umn.edu/bitstream/handle/11299/151329/1/Mn_DOT2008-11.pdf) (Accessed 22 Feb 2021)

International Institute for Applied Systems Analysis 2018 SSP database: version 2.0 (available at: https://tntcat.iiasa.ac.at/SspDb) (Accessed 22 February 2021)

Jiang L and O'Neill B C 2017 Global urbanization projections for the shared socioeconomic pathways *Glob. Environ. Change* **42** 193–9

Jiang L, O'Neill B C, Zoraghein H and Dahlke S 2020 Population scenarios for U.S. states consistent with shared socioeconomic pathways *Environ. Res. Lett.* **15** 094097

Jones B 2020 Modeling climate change-induced migration in central America & Mexico Methodological Report (available at: https://assets-c3.propublica.org/Climate-Migration-Modeling-Methodology.pdf) (Accessed 15 March 2021)

Jones B and O'Neill B C 2013 Historically grounded spatial population projections for the continental United States *Environ. Res. Lett.* **8** 044021

Jones B and O'Neill B C 2016 Spatially explicit global population scenarios consistent with the shared socioeconomic pathways *Environ. Res. Lett.* **11** 084003

Jones B, O'Neill B C, McDaniel L, McGinnis S, Mearns L O and Tebaldi C 2015 Future population exposure to US heat extremes *Nat. Clim. Change* **5** 652–5

Jones B, Tebaldi C, O'Neill B C, Oleson K and Gao J 2018 Avoiding population exposure to heat-related extremes: demographic change vs climate change *Clim. Change* **146** 423–37

Jongman B, Winsemius H C, Aerts J C J H, Coughlan De Perez E, Van Aalst M K, Kron W and Ward P J 2015 Declining vulnerability to river floods and the global benefits of adaptation *Proc. Natl Acad. Sci. USA* **112** E2271–80

Kc S and Lutz W 2017 The human core of the shared socioeconomic pathways: population scenarios by age, sex and level of education for all countries to 2100 *Glob. Environ. Change* **42** 181–92

Koomen E and Diogo V 2017 Assessing potential future urban heat island patterns following climate scenarios, socio-economic developments and spatial planning strategies *Mitigation Adapt. Strateg. Glob. Change* **22** 287–306

Kriegler E, Edmonds J, Hallegatte S, Ebi K L, Kram T, Riahi K, Winkler H and Van Vuuren D P 2014 A new scenario framework for climate change research: the concept of shared climate policy assumptions *Clim. Change* **122** 401–14

Kummu M, De Moel H, Salvucci G, Viviroli D, Ward P J and Varis O 2016 Over the hills and further away from coast: global geospatial patterns of human and environment over the 20th–21st centuries *Environ. Res. Lett.* **11** 34010

Lange M A, Llasat M C, Snoussi M, Graves A, Le Tellier J, Queralt A and Vagliasindi G M 2020 Introduction *Climate and Environmental Change in the Mediterranean Basin—Current Situation and Risks for the Future: First Mediterranean Assessment Report* ed W Cramer *et al* (Marseille, France)

Leimbach M, Kriegler E, Roming N and Schwanitz J 2017 Future growth patterns of world regions—A GDP scenario approach *Glob. Environ. Change* **42** 215–25

Leyk S *et al* 2019 The spatial allocation of population: a review of large-scale gridded population data products and their fitness for use *Earth Syst. Sci. Data* **11** 1385–409

Lincke D and Hinkel J 2018 Economically robust protection against 21st century sea-level rise *Glob. Environ. Change* **51** 67–73

Lückenkötter J, Hurth F and Schonlau M 2017 *European Population Projections for 2015–2060: 10-kmGridded Data Based on the Shared Socioeconomic Pathways (SSPs)* (IRPUD, TU Dortmund)

Marsha A, Sain S R, Heaton M J, Monaghan A J and Wilhelmi O V 2018 Influences of climatic and population changes on heat-related mortality in Houston, Texas, USA *Clim. Change* **146** 471–85

McGranahan G, Balk D and Anderson B 2007 The rising tide: assessing the risks of climate change and human settlements in low elevation coastal zones *Environ. Urban.* **19** 17–37

McLeman R 2019 International migration and climate adaptation in an era of hardening borders *Nat. Clim. Change* **9** 911–8

MedECC 2020 Summary for policymakers *Climate and Environmental Change in the Mediterranean* Basin—Current Situation and Risks for the Future: First Mediterranean Assessment Report ed W Cramer *et al* (Marseille, France)

Merkens J-L, Lincke D, Hinkel J, Brown S and Vafeidis A T 2018 Regionalisation of population growth projections in coastal exposure analysis *Clim. Change* **151** 413–26

Merkens J-L, Reimann L, Hinkel J and Vafeidis A T 2016 Gridded population projections for the coastal zone under the shared socioeconomic pathways *Glob. Planet. Change* **145** 57–66

Merkens J-L and Vafeidis A 2018 Using information on settlement patterns to improve the spatial distribution of population in coastal impact assessments *Sustainability* **10** 3170

Monaghan A J, Sampson K M, Steinhoff D F, Ernst K C, Ebi K L, Jones B and Hayden M H 2018 The potential impacts of 21st century climatic and population changes on human exposure to the virus vector mosquito Aedes aegypti *Clim. Change* **146** 487–500

Moss R H *et al* 2010 The next generation of scenarios for climate change research and assessment *Nature* **463** 747–56

Murakami D and Yamagata Y 2019 Estimation of gridded population and GDP scenarios with spatially explicit statistical downscaling *Sustainability* **11** 2106

Neumann B, Vafeidis A T, Zimmermann J and Nicholls R J 2015 Future coastal population growth and exposure to sea-level rise and coastal flooding–a global assessment *PLoS One* **10** e0118571

Nicholls R J, Wong P P, Burkett V, Woodroffe C D and Hay J 2008 Climate change and coastal vulnerability assessment: scenarios for integrated assessment *Sustain. Sci.* **3** 89–102

O'Neill B C *et al* 2017 The roads ahead: narratives for shared socioeconomic pathways describing world futures in the 21st century *Glob. Environ. Change* **42** 169–80

O'Neill B C *et al* 2020 Achievements and needs for the climate change scenario framework *Nat. Clim. Change* **10** 1074–84

O'Neill B C, Kriegler E, Riahi K, Ebi K L, Hallegatte S, Carter T R, Mathur R and Van Vuuren D P 2014 A new scenario framework for climate change research: the concept of shared socioeconomic pathways *Clim. Change* **122** 387–400

Pesaresi M, Florczyk A, Schiavina M, Melchiorri M and Maffenini L 2019 GHS settlement grid, updated and refined REGIO model 2014 in application to GHS-BUILT R2018A and GHS-POP R2019A, multitemporal (1975–1990-2000-2015), R2019A (available at: http://data.europa.eu/89h/42e8be89-54ff-464e-be7b-bf9e64da5218) (Accessed 22 February 2021)

Pesaresi M, Melchiorri M, Alice S and Kemper T 2016 Atlas of the human planet 2016: mapping human presence on earth with the global human settlement layer (EUR, Scientific and technical research series vol 28116) (Luxembourg: Publications Office)

Preston B L, Yuen E J and Westaway R M 2011 Putting vulnerability to climate change on the map: a review of approaches, benefits, and risks *Sustain. Sci.* **6** 177–202

R Core Team 2020 *R: A Language and Environment for Statistical Computing* (Vienna, Austria: R Foundation for Statistical Computing)

Reimann L, Jones B, Nikoletopoulos T and Vafeidis A T 2021 Gravity-based population projections consistent with the SSPs. Figshare (https://doi.org/10.6084/m9.figshare.12451949)

Reimann L, Merkens J-L and Vafeidis A T 2018 Regionalized shared socioeconomic pathways: narratives and spatial population projections for the Mediterranean coastal zone *Reg. Environ. Change* **18** 235–45

Reimann L, Vollstedt B, Koerth J, Tsakiris M, Beer M and Vafeidis A T 2021 Extending the shared socioeconomic pathways (SSPs) to support local adaptation planning—a climate service for Flensburg, Germany *Futures* **127** 102691

Rich D C 1980 *Potential Models in Human Geography* (*Concepts and techniques in modern geography* vol 26) (Norwich: Geo Abstracts)

Rigaud K K *et al* 2018 *Groundswell: Preparing for Internal Climate Migration* (Washington, DC: The World Bank)

Rohat G, Flacke J, Dosio A, Dao H and Maarseveen M 2019a Projections of human exposure to dangerous heat in African cities under multiple socioeconomic and climate scenarios *Earth's Future* **7** 528–46

Rohat G, Flacke J, Dosio A, Pedde S, Dao H and Van Maarseveen M 2019b Influence of changes in socioeconomic and climatic conditions on future heat-related health challenges in Europe *Glob. Planet. Change* **172** 45–59

Rohat G, Wilhelmi O, Flacke J, Monaghan A, Gao J, Dao H and Van Maarseveen M 2019c Characterizing the role of socioeconomic pathways in shaping future urban heat-related challenges *Sci. Total Environ.* **695** 133941

Schiavina M, Freire S and MacManus K 2019 GHS population grid multitemporal (1975, 1990, 2000, 2015) R2019A (available at: http://data.europa.eu/89h/0c6b9751-a71f-4062-830b-43c9f432370f) (Accessed 22 February 2021)

Seto K C, Fragkias M, Güneralp B and Reilly M K 2011 A meta-analysis of global urban land expansion *PLoS One* **6** e23777

Skov-Petersen H 2001 Estimation of distance-decay parameters: GIS-based indicators of recreational accessibility *ScanGIS* pp 237–58

Tatem A J 2017 WorldPop, open data for spatial demography *Sci. Data* **4** 170004

Tiggeloven T *et al* 2020 Global-scale benefit–cost analysis of coastal flood adaptation to different flood risk drivers using structural measures *Nat. Hazards Earth Syst. Sci.* **20** 1025–44

United Nations, Department of Economic and Social Affairs, Population Division 2019 *World Urbanization Prospects: The 2018 Revision* (New York: United Nations)

Vafeidis A T, Nicholls R J, McFadden L, Tol R S J, Hinkel J, Spencer T, Grashoff P S, Boot G and Klein R J T 2008 A new global coastal database for impact and vulnerability analysis to sea-level rise *J. Coast. Res.* **244** 917–24

Van Ruijven B J *et al* 2014 Enhancing the relevance of shared socioeconomic pathways for climate change impacts, adaptation and vulnerability research *Clim. Change* **122** 481–94

Van Vuuren D P *et al* 2011 The representative concentration pathways: an overview *Clim. Change* **109** 5–31

Van Vuuren D P *et al* 2014 A new scenario framework for climate change research: scenario matrix architecture *Clim. Change* **122** 373–86

Van Vuuren D P, Smith S J and Riahi K 2010 Downscaling socioeconomic and emissions scenarios for global environmental change research: a review *WIREs Clim. Change* **1** 393–404

Vanos J K, Baldwin J W, Jay O and Ebi K L 2020 Simplicity lacks robustness when projecting heat-health outcomes in a changing climate *Nat. Commun.* **11** 6079

Veldkamp T I E, Wada Y, Aerts J C J H and Ward P J 2016 Towards a global water scarcity risk assessment framework: incorporation of probability distributions and hydro-climatic variability *Environ. Res. Lett.* **11** 024006

Voros J 2003 A generic foresight process framework *Foresight* **5** 10–21

Walker W, Haasnoot M and Kwakkel J 2013 Adapt or perish: a review of planning approaches for adaptation under deep uncertainty *Sustainability* **5** 955–79

Winsemius H C *et al* 2016 Global drivers of future river flood risk *Nat. Clim. Change* **6** 381–5

Yamazaki D, Ikeshima D, Tawatari R, Yamaguchi T, O'Loughlin F, Neal J C, Sampson C C, Kanae S and Bates P D 2017 A high-accuracy map of global terrain elevations *Geophys. Res. Lett.* **44** 5844–5

Zoraghein H and O'Neill B C 2020a U.S. State-level projections of the spatial distribution of population consistent with shared socioeconomic pathways *Sustainability* **12** 3374

Zoraghein H and O'Neill B 2020b A spatial population downscaling model for integrated human-environment analysis in the United States *Demogr. Res.* **43** 1483–526